文章编号：1001-9014(2020)01-0001-05

DOI:10. 11972/j. issn. 1001-9014. 2020. 01. 001

The influence of annealing temperature on the structure and optical properties of silicon films deposited by electron beam evaporation

LIU Bao-Jian, DUAN Wei-Bo*, LI Da-Qi, YU De-Ming, CHEN Gang, LIU Ding-Quan

(Shanghai Institute of Technical Physics, Chinese Academy of Sciences, Shanghai 200083, China)

Abstract: In this paper, the influence of annealing temperature on the structure and optical properties of silicon films was systemically investigated. Silicon films were deposited by electron beam evaporation and then annealed in N_2 atmosphere within a temperature range from 200 to 500 °C. The films were characterized by X-ray diffraction (XRD), Raman spectroscopy, electronic-spin resonance (ESR) and optical transmittance measurement, respectively. With annealing temperature increased, the amorphous network order of silicon films was improved on the short and medium range and the defect density decreased remarkably. When sample being annealed at 400°C, the extinction coefficient k decreased from 6.14×10^{-3} to a minimum value of 1.02×10^{-3} (at 1000 nm), which was due to the lowest defect density, about one fifth of the as-deposited sample. The results showed that annealing at an appropriate temperature could effectively reduce the optical absorption of silicon films in the near infrared region, which were very critical for the application in optical thin film coating devices.

Key words: optical coatings, silicon films, optical properties, annealing

PACS: 42. 79. Wc, 78. 20. -e, 81. 40. Ef

退火温度对电子束蒸发沉积硅薄膜结构和光学性能的影响

刘保剑, 段微波*, 李大琪, 余德明, 陈 刚, 刘定权

(中国科学院上海技术物理研究所,上海 200083)

摘要:系统研究了退火温度对硅薄膜结构和光学性能的影响。通过电子束蒸发工艺制备硅薄膜,然后在氮气保护下对薄膜样品在200～500°C范围内进行退火处理。使用XRD、拉曼光谱、电子自旋共振和透射光谱测量等方法对薄膜样品进行了表征。结果显示,随着退火温度的升高,非晶硅薄膜结构有序度在短程和中程范围内得到改善,同时缺陷密度显著降低。当样品在400°C退火后,消光系数k由6.14×10^{-3}下降到最小值1.02×10^{-3}(1000 nm),这是由于此时硅薄膜缺陷密度也降到最低,约为沉积态薄膜的五分之一。试验结果表明,硅薄膜在适当的温度下退火可以有效地降低近红外区膜层的光学吸收,这对硅薄膜在光学薄膜器件研制中具有重要应用。

关 键 词:光学薄膜;硅薄膜;光学性能;退火

中图分类号:O484.4 **文献标识码**:A

Introduction

The optical constants of optical thin films, like refractive index and extinction coefficient, are important factors that directly affect the design and preparation of optical thin films. In the Fabry-Perot (F-P) filters, at a given membrane structure, increasing the ratio of the high and low refractive index, can narrow the passband width and expand the cut-off band width[1-2]. The short-wave infrared region (0. 75~2. 5 μm) is the transition region between the visible and infrared regions. High refractive index materials commonly used in the visible region, such as Ta_2O_5, Nb_2O_5 and TiO_2, can be applied to this band. Nevertheless, the number of film layers in the F - P filter is high on account of the low refractive index, and consequently coating time greatly enhances. At the same time, the out-of-band rejection of filter is difficult

Received date: 2019- 04- 17, **revised date**: 2019- 11- 19 **收稿日期**:2019- 04- 17,**修回日期**:2019- 11- 19

Foundation items: Supported by the National Natural Science Foundation of China (61605229); Innovation Program of Shanghai Institute of Technical Physics, Chinese Academy of Sciences (CX-129)

Biography: LIU Bao-Jian (1988-), male, Handan, master. Research area involves thin film optics and technology. E-mail: liubaojian@mail. sitp. ac. cn.

* **Corresponding author**: E-mail: duanweibo@mail. sitp. ac. cn

to deal with, which makes the optical coating design more difficult. Silicon thin film materials can overcome the shortcomings of the oxide materials in the shortwave infrared band. Silicon films have been widely used in the field of infrared optical thin films for its many advantages, such as high refractive index, good transparency, high stability and so on[3-4]. Although electron beam evaporation has been extensively applied to prepare silicon thin films, the absorption of silicon film is relatively high, especially in the near infrared region with wavelengths less than 1.5μm. Annealing can be taken as an effective method to improve film packed density and reduce defects[5-7], so as to improve the optical performance of thin films.

Some papers concerned the influence of annealing on optical properties and structure of a-Si:H films[8-12]. Wang et al. [10] reported the small vacancy-type defects coalesced in a-Si thin film around 450°C and the a-Si crystallized near 650°C. Goh Boon Tong et al. [11] studied the effect of annealing on optical properties of Si:H thin film deposited by layer-by-layer (LBL). When annealed at the transition temperature of 600 °C, the films with the highest refractive index had the most disordered structure. Therefore, it was speculated that annealing could further reduce optical absorption, yielding to improve the optical performance of silicon films. However, few papers researched the influence of annealing on the structure and optical properties of silicon films deposited by electron beam evaporation. Moreover, seldom studies further investigated of the relationship between structure of silicon films and the optical properties in the near infrared region, which were very critical for the application of silicon film in optical thin film coating devices.

In this paper, the influence of annealing temperature on the structure and optical properties of silicon films was systemically investigated. Silicon films were deposited by electron beam evaporation and then annealed in N_2 ambience within 200 ~ 500 °C. The films were characterized by XRD, Raman spectroscopy, ESR and optical transmittance measurement, respectively.

1 Experimental

1.1 Film preparation

Silicon films were deposited by electron beam evaporation on sapphire substrates under identical conditions. Before deposition, the specimens with dimensions of Φ 10×1 mm were cleaned with ethyl ether alcohol solution. During silicon films growth, the temperature of substrates was keeping 250°C. The silicon films were deposited by the evaporation rate of 0.4 nm/s at a base pressure of 1×10^{-3}Pa. The film deposition time was approximately 45 minutes. After deposition, the samples were annealed for 1h in N_2 atmosphere. Annealing temperatures were 200°C, 300°C, 400°C and 500°C, respectively. The temperatures were heightened to desired level gradually.

1.2 Film characterization

The X-ray diffractometer (XRD) was wielded to investigate the structure of silicon films by Cu-target Kα radiation at 40 kV in the scanning angular from 10° to 80° at 2°/min. The Raman spectra were acquired to estimate the evolution of network structure through Micro Raman Spectrometer with the HeCd laser beam at 532 nm. The ESR measurement was performed by a double-cavities BRUKER ESP4105 spectrometer operated by X-band microwave radiation with a power of 20 mW at 80 K. Via a Lambda 900 spectrophotometer, the transmission spectrum of silicon films were measured and the measurement error was within 0.08%. From transmittance spectra, the refractive index (n) and extinction coefficient (k) of silicon films were calculated by using the Cauchy Exponential Model. In the dispersion model, the absorption coefficient varied exponentially with frequency. This allowed the Cauchy Exponential to model a large variation in the value of k versus wavelength. The following formulas were used to define the optical constants[13-14]:

$$n(\lambda) = A_n + \frac{B_n}{\lambda^2} + \frac{C_n}{\lambda^4} \quad , \quad (1)$$

$$k(\lambda) = A_k Exp\left(B_k\left(\frac{1.2398}{\lambda} - C_k\right)\right) \quad , \quad (2)$$

where λ is wavelength, A_n, B_n, and C_n are material coefficients, A_k is amplitude, B_k is the exponent factor and C_k is the band edge.

2 Results and discussion

2.1 Structure of silicon films

As shown in Fig. 1, XRD measurement was utilized to investigate the structural transformation of as-deposited silicon film and those upon annealing at different temperatures. It was clearly identified that all silicon films were amorphous in structure, because no obvious diffraction peak was found, which indicated that silicon film was not crystallized at 500°C. These results very closely corresponded to the report of Goh Boon Tong et al. [11], which showed that the structure of silicon film changed from amorphous to crystalline phase, when hydrogenated silicon films annealed at 800°C. An intensive research to the evolution of network structure could be achieved by the analysis of Raman spectra.

The widespread usage of Raman scattering into the research of microstructure materials lied in the fact that

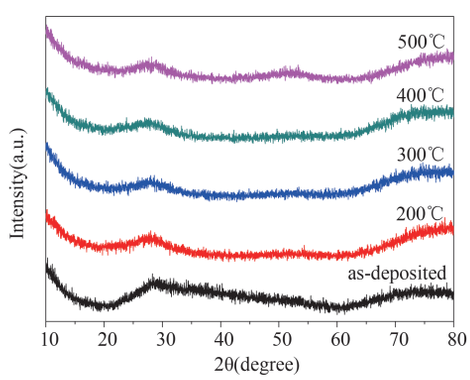

Fig. 1 XRD patterns of silicon films annealed at different temperatures.
图1 硅薄膜经过不同温度退火后的XRD谱图

its intensity was susceptible to the order degree of solid structure. The Raman spectra of as-deposited and annealed silicon films were shown in Fig. 2(a). The Gauss-deconvolution result of silicon film annealed at 400°C was shown in Fig. 2(b). It could be discovered that all Raman spectrum contained several vibration modes, including the transverse optical mode (*TO*), transverse acoustic mode (*TA*), longitudinal optical mode (*LO*) and longitudinal acoustic mode (*LA*)[15]. Table 1 stated the corresponding characteristic parameters. As we could see, the broad *TO* peaks were approximately at 480 cm^{-1}, which was sensitive to the amorphous network order on short-range scales[16]. This further confirmed the amorphous structure of silicon films after annealing. Meanwhile, the *TO* peak width Γ_{TO} decreased from 68.4 to 65.9 cm^{-1}, which showed the enhancement of short-range order in silicon films with annealing temperature increased. The *TA* mode at about 150 cm^{-1} associated with the amorphous network order on medium-range scales[17]. In addition, while the annealing temperature went up, the intensity ratio I_{TA}/I_{TO} decreased from 0.670 to 0.478, which indicated the improvement of medium-range order. The *LO* mode at about 410 cm^{-1} along with the *LA* mode at 300 cm^{-1} were connected to the coordination defects in silicon films. Moreover, where there were more defects, the values of I_{LA}/I_{TO} as well as I_{LO}/I_{TO} became larger[18]. As shown in Table 1, before and after annealing, I_{LA}/I_{TO} decreased from 1.02 to 0.678 and I_{LO}/I_{TO} from 0.358 to 0.331, reflecting the decrease of defects. These results indicated that the structure of silicon films maintained amorphous, but, with rise of temperature, the amorphous network order was improved in the short and medium range.

Table 1 Raman characteristic parameters of the as-deposited and annealed silicon films
表1 沉积态和退火后硅薄膜的拉曼光谱特征参数

Annealing temperature (°C)	Γ_{TO} (cm^{-1})	I_{LA}/I_{TO}	I_{LO}/I_{TO}	I_{TA}/I_{TO}
as-deposited	68.4	1.02	0.358	0.670
200	67.4	0.718	0.352	0.592
300	66.7	0.711	0.334	0.524
400	66.4	0.678	0.331	0.481
500	65.9	0.690	0.350	0.478

ESR was among few experiments offered defects information in structure[19]. Fig. 3 illustrated the derivative ESR spectrum of silicon films, *g* factor and density of dangling bonds (*Ns*) at different annealing temperatures. It could be discovered that *g* factor values of all silicon films were around 2.0055, which originated from the dangling bonds in amorphous structure[20]. It was worth noting that when the annealing temperature increased, the strength of resonance signals decreased obviously. As shown in Fig. 3, *Ns* decreased from 1.1×10^{17} cm^{-3} for as-deposited sample to a minimum of 3.4×10^{16} for sample annealed at 400°C. It showed the rise of annealing temperature could reduce, to a large extent,

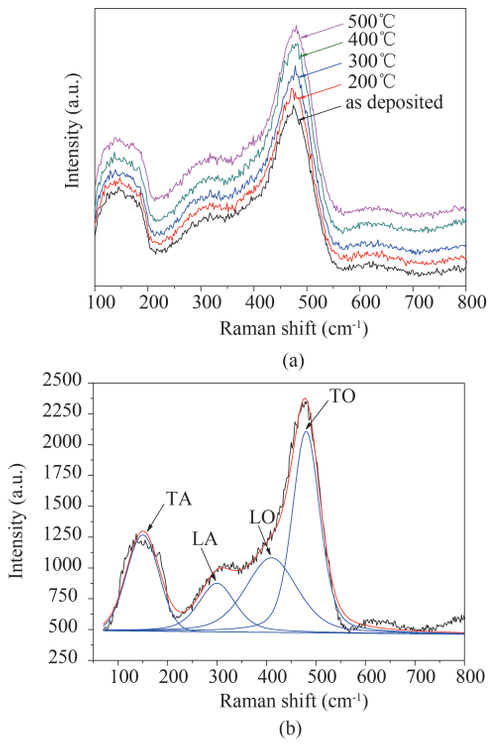

Fig. 2 (a) Raman spectra of the as-deposited and annealed silicon films; (b) The Gauss-deconvolution of Raman spectrum for silicon film annealed at 400 °C.
图2 (a) 沉积态和退火后的硅薄膜拉曼光谱;(b) 400°C退火后的硅薄膜拉曼光谱分峰谱图

the dangling bonds in silicon films. It almost accorded with the result obtained by Raman scattering.

2.2 Optical properties of silicon films

Fig. 4 described the transmittance spectra of as-deposited and annealed silicon films from 800 to 2 000 nm.

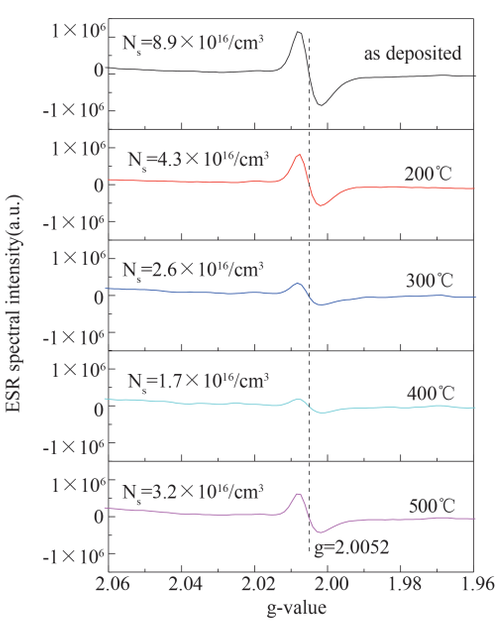

Fig. 3 Derivative ESR spectra of the as-deposited and annealed silicon films
图3 沉积态和退火后的硅薄膜ESR谱图

The transmittance spectrum of silicon films exhibited peaks and valleys that were associated with interference effects. Along with annealing temperature heightened, the optical transmittance spectra shifted to a shorter wavelength due to the reduction of film optical thicknesses. When annealed at 400° C, the sample showed higher peak transmittance than those of films annealed at other temperatures, especially from 800nm to 1 200 nm band. This result indicated a notable decrease of optical absorption with the rise of annealing temperature. Fig. 5 showed the plots of the films optical and physical thickness against annealing temperature calculated from transmittance spectra. As could be seen, when annealed at 200~300° C, the variation on physical thickness of silicon film was not obvious. But when annealed at a higher temperature (300~500 °C), the physical thickness rapidly decreased from 1104. 4 nm to 1 071. 4 nm, indicating that the film packing density was greatly improved. This might be because, as annealing temperature increased, the heated atoms were filled into the voids and diffused each other, which made the film compact and thus reduced the thickness.

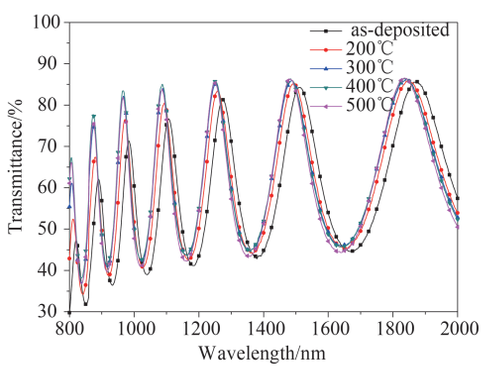

Fig. 4 Optical transmittance spectra of as-deposited silicon film and the silicon films annealed at different temperatures.
图4 沉积态硅薄膜和经过不同温度退火后的硅薄膜透射光谱

The optical constants of silicon films were fitted by using the FilmWizard software from SCI. During fitting process, the Cauchy Exponential Model was used as the dispersion model of material to fit the transmission spectrum. Table 2 stated the dispersion model parameters of the as-deposited and annealed silicon films, which could be used to describe the variation of optical constants. Fig. 6(a) showed the refractive index n of the as-deposited and annealed silicon films. From the figure, it could be evidently found that the refractive index decreased

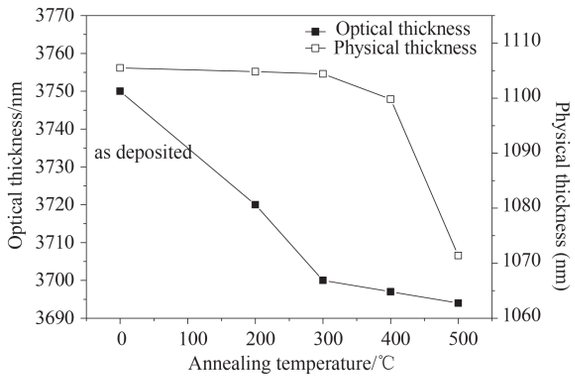

Fig. 5 Variation of film optical thickness and physical thickness with annealing temperatures.
图5 硅薄膜光学厚度和物理厚度随退火温度的变化

with adding wavelength of the incident light. Along with annealing temperature increased, the refractive index n of silicon films initially declined and then rose at a specific wavelength. For example, the refractive index n decreased from 3. 52 for as-deposited sample to 3. 48 for sample annealed at 300°C and went up to 3. 58 at 500°C (at 1 000 nm). The decrease of n was probably associated with the decrease in the number of dangling bonds. When annealed at a higher temperature (300~500°C), it was the packing density, though still along with changes in dangling bond density, that became the main factor affecting the variation in refractive index. Thermal annealing could remarkably improve the packing density of silicon films, which had been confirmed by the decrease of physical thickness.

Fig. 6(b) presented the extinction coefficients k of the as-deposited and annealed silicon films. From the figure, it could be obviously found that after annealing extinction coefficient k decreased apparently, especially in the near infrared region with wavelengths less than 1. 5μm. For instance, the extinction coefficient k dropped from 6.14×10^{-3} for as-deposited sample to 1.02×10^{-3} for sample annealed at 400°C (at 1 000 nm). It was interesting to notice that the extinction coefficient and film defect density possessed similar variation tendency. The extinction coefficient k also decreased initially to its minimum value at 400 °C and increased by rising annealing temperature further. Therefore, the decrease of extinction coefficient might be attributed to the decline in the number of dangling bonds in silicon films.

Table 2 Dispersion model parameters of the as-deposited and annealed silicon films
表2 沉积态和退火后硅薄膜的色散模型参数

Annealing temperature (°C)	A_n	B_n	C_n	A_k	B_k	C_k
as-deposited	3. 322	0. 143	0. 059	4.088×10^{-5}	4. 858	0. 228
200	3. 304	0. 124	0. 068	1.349×10^{-5}	5. 680	0. 229
300	3. 293	0. 112	0. 073	1.328×10^{-6}	7. 117	0. 232
400	3. 302	0. 111	0. 074	4.136×10^{-7}	7. 861	0. 245
500	3. 386	0. 119	0. 076	8.843×10^{-7}	7. 509	0. 271

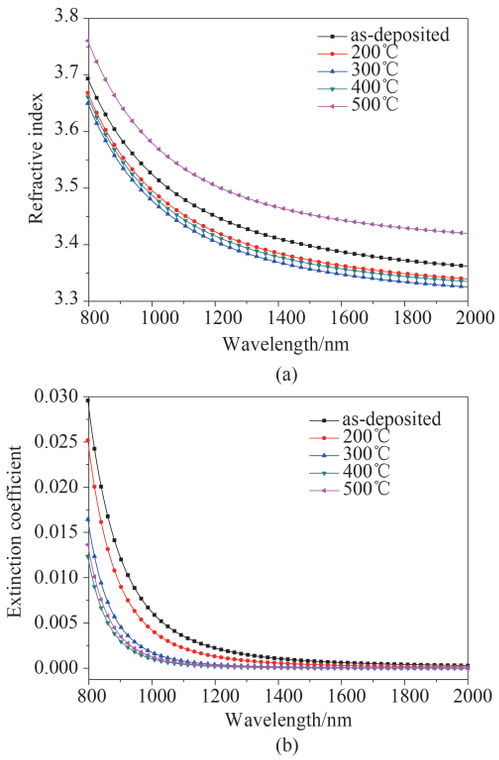

Fig.6 Dispersion of (a) refractive index, (b) extinction coefficient of the as-deposited and annealed silicon films
图6 (a)沉积态和退火后硅薄膜的折射率(b)消光系数的色散曲线

3 Conclusion

The silicon films were deposited on sapphire wafer by electron beam evaporation and then annealed in N_2 atmosphere in a temperature range from 200 to 500 °C. It was concluded that all silicon films maintained amorphous in microstructure, but with annealing temperature increased, the amorphous network order was improved on the short and medium range. Meanwhile, the defect concentration from ESR measurement decreased distinctly. When sample being annealed at 400° C, the defect density declined to the minimum, about one fifth of the as-deposited sample. With annealing temperature increased, transmittance spectra of silicon films shifted to the shorter wavelength direction, owing to the decrease of film thickness and the change of refractive index. When sample being annealed at 400°C, extinction coefficient also cut down to the minimum, and then mounted up by rising annealing temperature further. According to these results, annealing at an appropriate temperature could effectively reduce the optical absorption of silicon films in the near infrared region, which were very critical for the application in optical thin film coating devices.

Acknowledgment

This work was supported by the Young Scientists Fund of the National Natural Science Foundation of China (Grant No. 61605229); Innovation Program of Shanghai Institute of Technical Physics, Chinese Academy of Sciences (Grant No. CX-129).

References

[1] Bruynooghe S. Optical properties of plasma ion-assisted deposition silicon coatings: application to the manufacture of blocking filters for the near-infrared region [J]. *Applied optics*, 2008, **47** (13): C47 - C48.
[2] Yoda H, Shiraishi K, Hiratani Y, *et al*. a-Si: H/SiO_2 multilayer films fabricated by radio-frequency magnetron sputtering for optical filters [J]. *Applied optics*, 2004, **43** (17): 3548 - 3554.
[3] Mao L, Ye H. New development of one-dimensional Si/SiO_2 photonic crystals filter for thermophotovoltaic applications [J]. *Renewable Energy*, 2010, **35** (1): 249 - 256.
[4] Gainutdinov I S, Nesmelov E A, Aliakberov R D, *et al*. Stabilization of the optical parameters of filters based on amorphous silicon [J]. *Journal of Optical Technology*, 2004, **71**(12):842 - 846.
[5] Long C S, Lu H H, Lii D F, *et al*. Effects of annealing on near-infrared shielding properties of Cs-doped tungsten oxide thin films deposited by electron beam evaporation [J]. *Surface & Coatings Technology*, 2015, **284**: 75 - 79.
[6] Woo S H, Hwangbo C K. Effects of annealing on the optical, structural, and chemical properties of TiO_2 and MgF_2 thin films prepared by plasma ion-assisted deposition [J]. *Applied optics*, 2006, **45** (7): 1447 - 1455.
[7] Khan A F, Mehmood M, Rana A M, *et al*. Effect of annealing on structural, optical and electrical properties of nanostructured Ge thin films [J]. *Applied Surface Science*, 2010, **256** (7): 2031 - 2037.
[8] Zarchi M, Ahangarani S. Study of silicon films deposited by EB-PVD and the effect of applying annealing conditions on them [J]. *Optik*, 2018, **154**: 601 - 609.
[9] Elghoul N, Kraiem S, Jemai R, *et al*. Annealing effects on electrical and optical properties of a-Si: H layer deposited by PECVD [J]. *Materials Science in Semiconductor Processing*, 2015, **40** (4): 302 - 309.
[10] Wang X N, He X Y, Mao W F, *et al*. Microstructure evolution of amorphous silicon thin films upon annealing studied by positron annihilation [J]. *Materials Science in Semiconductor Processing*, 2016, **56**: 344 - 348.
[11] Tong G B, Muhamad M R, Rahman S A. Optical properties of annealed Si: H thin film prepared by layer-by-layer (LBL) deposition technique [J]. *Physica B*, 2010, **405** (23): 4838 - 4844.
[12] Netrvalová M, Vavruňková V, Müllerová J, *et al*. Optical properties of re-crystallized polycrystalline silicon thin films from a-Si films deposited by electron beam evaporation [J]. *Journal of Electrical Engineering*, 2009, **60**(5): 279 - 282.
[13] Fujiwara H. Spectroscopic Ellipsometry: Principles and Applications [M]. West Sussex: John Wiley & Sons Ltd, 2007.
[14] Amin M S, Hozhabri N, Magnusson R. Effects of solid phase crystallization by rapid thermal annealing on the optical constants of sputtered amorphous silicon films [J]. *Thin Solid Films*, 2013, **545** (18): 480 - 484.
[15] He J, Wang C, Li W, *et al*. Effect of gas temperature on the structural and optoelectronic properties of a-Si: H thin films deposited by PECVD [J]. *Surface & Coatings Technology*, 2013, **214** (2): 131 - 137.
[16] Marinov M, Zotov N. Model investigation of the Raman spectra of amorphous silicon [J]. *Physical Review B*, 1997, **55**(5): 2938 - 2944.
[17] Wei W S, Xu G Y, Wang J L, *et al*. Raman spectra of intrinsic and doped hydrogenated nanocrystalline silicon films [J]. *Vacuum*, 2007, **81** (5): 656 - 662.
[18] Zotov N, Marinov M, Mousseau N, *et al*. Dependence of the vibrational spectra of amorphous silicon on the defect concentration and ring distribution [J]. *Journal of Physics Condensed Matter*, 1999, **11**: 9647 - 9658.
[19] Street R A. Hydrogenated Amorphous Silicon [M]. Cambridge: Cambridge University Press, 1991.
[20] Astakhov O, Carius R, Lambertz A, *et al*. Structure of the ESR spectra of thin film silicon after electron bombardment [J]. *Journal of Non-Crystalline Solids*, 2008, **354** (19 - 25): 2329 - 2332.